HEAVY METAL CONTAMINATION AND RISK ASSESSMENT OF GROUNDWATER IN JALINGO VULNERABLE AREA, NIGERIA: A MULTI-METHOD APPROACH

Ngasoh, F.G.[1*], Ankidawa, B.A.[2] and Burmamu B.R.[2]

[1]Department of Agricultural and Bioresources Engineering, Taraba State University, Jalingo

[2]Department of Agricultural and Environmental Engineering, Modibbo Adama University, Yola

*Corresponding email: felixngasoh@gmail.com

ABSTRACT

Heavy metal contamination of groundwater in Jalingo, Nigeria, threatens public health and ecosystem services, driven by both natural geologic sources and intensive local anthropogenic activities. This study aimed to apply a multi-method approach to quantify heavy-metal levels, map spatial patterns, assess contamination and ecological risk, and predict pollution risk classes to inform management. Water was collected by purge-and-sample from vulnerable open wells, preserved with HNO_3, and analysed by Atomic Absorption Spectroscopy for 11 metals (Pb, Hg, Cd, As, Cr, Ni, Mn, Zn, Cu, Co, Fe). Statistical and geospatial methods, which include Kernel Density Estimation (KDE), Pearson correlation, contour mapping (Surfer v28), Metal Index (MI), and Degree of Contamination (DoC) were combined with a Support Vector Machine (SVM) model to predict a Heavy Pollution Index Risk Factor (HPI-RF) using a 72/28 percent train-test split. Results show widespread exceedances of WHO limits for several metals (e.g., mean Pb ≈1.21 mg/L vs. 0.01 mg/L guideline; Cu mean ≈4.03 mg/L; As mean ≈0.90 mg/L; Fe mean ≈3.48 mg/L; Mn ≈1.85 mg/L; Ni and Zn with localized maxima far above limits). KDE and maps revealed distinct contamination hotspots (As-NW, Pb-NE, Cu-east, Ni-south-central, Mn-central-SE, Hg-SE). Strong positive correlations among Pb, Cd, Cr, Hg, and Zn suggest a common source. SVM classified 25 sites into 12 high-risk, 2 medium-risk, and 11 low-risk locations, with an overall accuracy of 87.5%, but noted limitations due to class imbalance. The study concludes that groundwater in several zones is unsafe for consumption and requires urgent action. Targeted monitoring and remediation of hotspots, improved waste and industrial effluent management, infrastructure upgrades, routine surveillance, and expanded sampling to enhance predictive models and risk management.

Keywords: Groundwater-Contamination, Heavy-Metals, Spatial-Distribution-Mapping, Pollution-Risk-Modelling

1 INTRODUCTION

The increasing global concerns regarding water quality have heightened the need for thorough evaluation and monitoring of groundwater resources, especially in areas vulnerable to pollution from human activities and natural geological factors [1]. The major sources of contamination may include industrial discharges, household wastewater, and agricultural runoff, as well as indiscriminate waste disposal, which significantly threaten both human health and ecological balance [2]. Even minimal amounts of heavy metals in water can seriously harm aquatic life, reduce agricultural output, and affect human well-

being [3]. Because of their high density and toxicity, heavy metals can persist in the environment for long periods, accumulate in the food chain, and pose long-term hazards [4]. These metals can sometimes disrupt the reproductive cycles, enzymatic functions, and metabolic processes of aquatic organisms within their habitat [5]. Investigating heavy metal pollution in groundwater is crucial for identifying the sources, pathways, and possible effects of these contaminants on water supplies. A detailed analysis of heavy metal pollution is essential for creating effective strategies to reduce contamination, safeguard public health, and ensure sustainable water resource management. Heavy metals in water sources pose significant threats to human health, leading to various adverse health outcomes [6]. In contrast to organic pollutants, heavy metals do not break down naturally, and their buildup in living organisms can cause toxic and carcinogenic effects [7]. Contact with heavy metals like lead, mercury, cadmium, and arsenic through polluted water can lead to serious health problems, such as neurological disorders, kidney damage, and various cancers [8]. These contaminants enter aquatic systems through industrial waste, mining activities, and agricultural methods [9]. The enduring and bioaccumulative characteristics of heavy metals are especially alarming since even minimal, continuous exposure can cause significant health issues, including cancer-related issues, immunosuppression, neurotoxicity, and liver toxicity [10]. The presence of heavy metals in water environments is a result of natural geological processes, soil erosion, and numerous human activities [5, 11]. Consequently, using water contaminated with heavy metals leads to increased rates of illness and death globally [12]. The fact that heavy metals are resistant to deterioration allows them to persist in the environment and biological organisms for extended periods [13]. The growth of industrial activity, mining operations, and environmental disasters linked to climate change has significantly contributed to the spread of harmful toxins in aquatic ecosystems, impacting water quality and human health [14, 15]. Till now, the issue of heavy metal contamination has become more pressing due to its potential to affect the environment and human health adversely [16]. By examining the concentrations of heavy metals like lead, cadmium, and arsenic, researchers can pinpoint pollution hotspots and evaluate the overall quality of groundwater resources [17]. Grasping the distribution and sources of these contaminants is key to the development and effective management strategies, consequentially reducing the negative impacts on public health and the environment [18]. Researchers globally adopt accepted indices for various assessments in surface and subsurface water sources [19], [20]. Qingjie and Jun [21] classified the indices to assess heavy metal contamination into three types: contamination indices, background enrichment indices, and ecological risk indices, while Bsiwas *et al.* [22] and Karaouzas *et al.* [20] checked pollution indices using three methods: heavy metal pollution index (HPI), Heavy metal evaluation index (HEI), and degree of contamination (C_d). The heavy metal pollution and evaluation indices methods provide an overall assessment of water quality for both irrigation and drinking. At the same time, the degree of contamination evaluates the extent of contamination. Karaouzas *et al.* [20] grouped HPI thus <100 (low), -1000 (medium), and >1000 (high). Similarly, [23] rated contamination as <4 (low), 4-8 (medium), and >8 (high). However, the aforementioned assessment methods could not capture risk-factor classification, clustering, and mapped the spatial distribution of the concentration. This research, therefore, aimed to apply a multi-method approach to analyse heavy metal contamination in an area vulnerable to contamination in Jalingo and environs. This approach anticipates potential contamination scenarios based on the pollution index. By foreseeing future risks, stakeholders can take proactive steps to protect groundwater resources.

2 MATERIALS AND METHODS

2.1 Study Area

Jalingo is situated in the north-eastern part of Nigeria at a latitude of 8 °.47’ N to 9 °.20’ N and longitude 11 °.13’E to 11 °.28’E. It has a landmass of 401.2 square kilometres, a population density of 550.1 per square kilometre, and an estimated annual population growth of 2.9% [24]. It consists of some localised industries and commercial activities that tend to generate waste. These includes: automobile repairs, rice milling, paint production, garri processing, agricultural activities that influence the use of herbicides/insecticides and fertilisers of all forms, etc. Figure 1 presents the map of the study area [25].

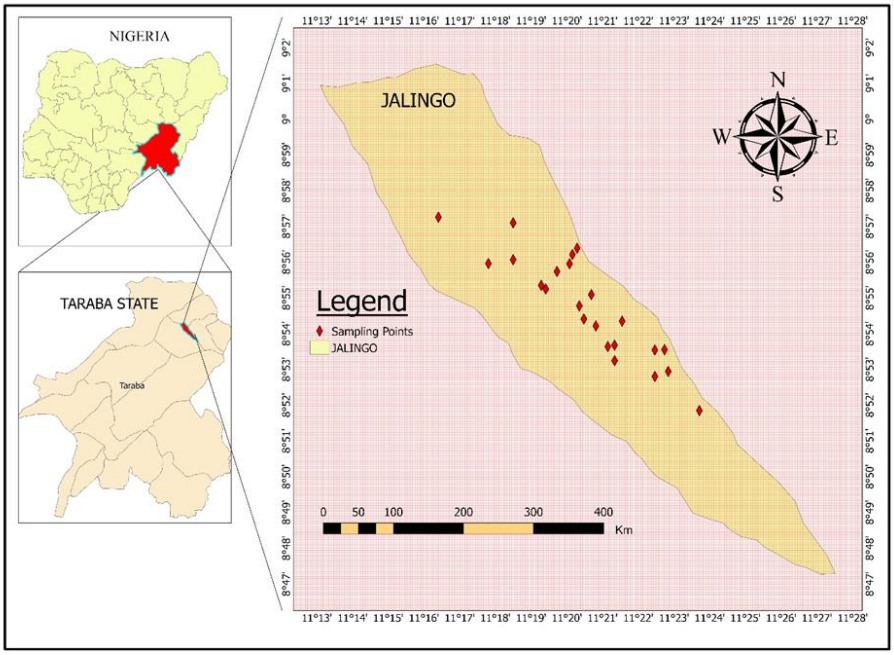

Figure 1. Map of study area [25]

2.2 Water Sample Collection

Water samples were collected from the study site around areas vulnerable to contamination. The purge-and-sample collection method was used to collect water from the wells or boreholes under investigation. This was achieved with a bailer bump for open wells. Samples that had. To preserve the samples, immediately after collection, the samples were preserved by adding 3 ml of concentrated nitric acid (HNO_3) to adjust the pH to below 2. This was done to prevent metal precipitation and adsorption onto the container walls. The added volume of acid was determined using a standard method and the sample [26].

2.2.1 Laboratory Analysis

The collected samples were packed in a cooling chamber and transported to Gombe State University for chemical analysis. Due to the high precision of Atomic Absorption Spectrometer (AAS) machine which is capable detecting in **parts per million (ppm) or even parts per billion (ppb), it was used to determine the concentration of the heavy metals in** eleven (11) chemical parameters, which includes; Lead (Pb), Mercury (Hg), Cadmium (Cd), Arsenic (As), Chromium (Cr), Nickel (Ni), Manganese (Mn), Zinc (Zn) Copper (Cu), cobalt (Co) and Iron (Fe). These were considered dangerous to humans and plants when present at concentrations above recommended levels.

2.2.2 Statistical Analysis

A Pearson's correlation Matrix was used to analyze the effects of individual heavy metals on one another. Meanwhile, clustering and spatial distribution were analysed using Kernel distribution estimation (KDE) via a Python code and Surfer version 28, respectively.

2.2.3 Metal and the degree of concentration index

The Metal Index (MI) is the combines concentrations of various metals found in the water into a single value, which helps determine whether the water is safe for drinking or other uses. This was calculated using Equation 1 [27].

$$MI = \sum_{i=1}^{n} \frac{C_i}{MAC_i} \quad (1)$$

Where; C_i= Concentration of ith metal in water (mg/L). MAC_i= Maximum Allowable Concentration for the ith metal (mg/L) as per WHO or national standards, n = Number of metals considered. The Degree of Contamination (DoC) is a valuable tool for evaluating how polluted water is due to various chemical factors, such as heavy metals. It gives a cumulative score that helps determine if the water is safe for drinking or other uses. This measurement was derived from 2 [23].

$$DoC = \sum_{i=1}^{n} C_{fi} = \frac{C_i}{MAC_i} - 1 \quad (2)$$

Where: C_i = measured concentration of ith parameter (mg/L). MAC_i = Maximum allowance concentration (WHO or national standard). n = Number of parameters.

2.2.4 Heavy pollution index risk factor (HPI-RF)

HPI-RF was predicted from the Computed Metal Index (MI) and Degree of Concentration (DoC). A Machine Learning (ML) model was built in an Anaconda-Python Environment using a support vector machine (SVM) algorithm. The machine was trained with 72% of the data, and the remaining 28% was used to test and predict the risk factor classification.

3 RESULTS AND DISCUSSION

3.1 Concentrate cluster and kernel density distribution

Figure 2 shows KDE plots that present a smooth, continuous view of the probability density function for each heavy metal concentration. This helps understand the level of contamination and the variability at different sampling points [28]. All the heavy metals exhibited significant right-skewed distributions suggesting that while most of the samples have relatively low concentration, only few exceptionally had high value. Lead (Pb) however, had average concentration of about 1.21 mg/L exceeds the WHO guideline limit of 0.01 mg/L by over 100% times. This trend indicates that although lead contamination may not be widespread, certain hotspots are present, due to localised anthropogenic activities such as deteriorating plumbing systems, battery disposal, or industrial emissions. The extended tail in the distribution points to wells that experience greater contaminant loading or are situated in areas of slower groundwater movement, where lead tends to accumulate over time. Similar observations were made by Chutia et al. [29], who noted that spatial variability and localised industrial impacts resulted in long-tailed lead distributions in vulnerable-urban groundwater systems. Cadmium (Cd) had a mean concentration of 0.77 mg/L and a pronounced peak at lower levels. The heavy right tail indicates that while numerous sites report moderate cadmium concentrations, a few significantly exceed safe limits. Cadmium's high mobility in acidic or oxidizing environments suggests that aquifers in areas with low pH or human activity, such as metal plating and waste disposal, may face increased contamination risks. This aligns with findings from Yang et al. [30], who indicated that nonparametric distribution analyses, such as KDE, can reveal outlier concentrations that traditional statistics may miss. The pronounced skewness of the cadmium distribution underscores the danger of localised exposure, particularly since cadmium is recognised for its bioaccumulative toxicity even at minimal levels [31]. Chromium (Cr) exhibits a comparatively narrower KDE curve in relation to lead and cadmium, with an average concentration of approximately 0.47 mg/L. The density peak is more concentrated, indicating that chromium contamination is more evenly distributed across the sampling sites. Nonetheless, the mean value remains significantly above the recommended threshold of 0.05 mg/L, suggesting possible contamination from sources such as industrial discharges or the weathering of chromium-containing earth materials. The limited dispersion of the KDE curve may imply that chromium is predominantly geogenic or less affected by specific anthropogenic sources. The mobility of chromium is largely dependent upon its oxidation state, and in numerous aquifers, the prevalence of Cr(III) over Cr(VI) restricts its spread. However, as noted by Xu et al. [32], even moderate levels of chromium in aquifers can present risks when redox conditions transition towards oxidizing states that facilitate Cr(VI) mobility. In contrast, mercury (Hg) displays a different trend, characterized by a sharp density peak around 0.1 mg/L and a relatively short tail extending towards higher concentrations. The concentration range is narrower, indicating reduced variability and suggesting that mercury inputs are more

dispersed or more evenly distributed. Despite the seemingly low concentrations, the high toxicity and bioaccumulation potential of mercury at this level are of public health concern. The modest dispersion of the KDE curve indicates limited point sources, such as small-scale artisanal operations, or geochemical conditions that trap mercury within the aquifer matrix [33]. Compared with other metals, mercury contamination appears less severe, which may be attributed to its tendency to adsorb onto sediments or organic matter rather than remaining in solution. However, despite its less severeness, when ingested either in its inorganic or organic form can be toxic and moderately absorbed through the gastrointestinal tract and finally accumulates in the kidney, consequentially causing damage to the organs [33], [34]. Nickel (Ni) shows similarities with lead and cadmium, with a moderate right-skewed distribution, a mean of 1.04 mg/L, and values up to 15 mg/L. The pattern indicates that while most groundwater samples contain relatively low nickel concentrations, a few exhibits considerably elevated levels. Nickel's mobility depends on pH and redox potential, and its higher values may correspond to zones where adsorption capacity is reduced or where industrial discharges contribute directly to groundwater [35]. The KDE profile suggests that nickel contamination, though not as extreme as zinc's, is still substantial and indicative of anthropogenic influence. Mohan et al. [36] also reported similar asymmetric distributions of nickel in riverine environments, attributing the spread to a mix of geogenic and anthropogenic inputs. The KDE plot for manganese (Mn) shows a unimodal distribution skewed to the right, with an average concentration of 1.85 mg/L. This figure is notably higher than the WHO guideline limit of 0.1 mg/L for drinking water [37]. The right-skewed distribution suggests that while most samples have lower Mn levels, a few outliers have very high concentrations, likely due to leaching from manganese-rich minerals or human activities such as waste disposal. High levels of Mn can affect water taste and may lead to neurological issues with long-term exposure [38]. Looking at copper (Cu), the distribution shows a sharp peak around the mean of 4.03 mg/L, with a long right tail extending to 50 mg/L. This right skew indicates that there are some areas with significant copper enrichment, possibly due to corroded pipes, industrial discharges, or mineralised zones [39]. The average concentration is well above the WHO permissible limit of 2.0 mg/L, raising concerns about potential health risks like gastrointestinal irritation and liver damage from prolonged consumption [17]. However, the KDE for cobalt (Co) shows a narrow, sharply peaked curve near the mean of 0.35 mg/L, indicating relatively low variability among the sampling points. However, this average still exceeds the typical background level of 0.05 mg/L for groundwater [40]. Elevated levels of Co may stem from industrial runoff or the weathering of mafic rocks, posing potential toxicity risks, including cardiomyopathy and thyroid dysfunction with chronic exposure [41]. This implies that areas with a high concentration of these heavy metals are at risk of ailments induced by their excess. Arsenic (As) displays a moderately right-skewed distribution with a mean value of 0.90 mg/L, which is significantly above the WHO standard of 0.01 mg/L [42]. This concerning concentration points to serious contamination, possibly linked to natural sources, such as the dissolution of arsenic-bearing minerals, or to human activities, such as pesticide use and waste disposal. The KDE curve indicates a widespread presence of As across the sampling sites, confirming findings from earlier studies by Owamah and Izinyon [43]. The distribution of iron (Fe) reveals an average concentration of 3.48 mg/L, which is significantly above the WHO's acceptable limit of 0.3 mg/L. This long right tail suggests that there are specific areas with very high Fe levels [32], likely caused by reducing groundwater conditions that release Fe^{2+} ions from ferric minerals [44]. While Fe is not considered highly toxic, its elevated levels can lead to water discolouration, unpleasant tastes, and even clogged pipes [45]. The KDE plots collectively reveal that groundwater contamination in the area is highly heterogeneous, with clear evidence of skewness and long tails for most metals. This heterogeneity suggests that contamination arises from a combination of diffuse and localised sources, interacting with variable hydrogeochemical conditions. Metals like Pb, Cd, Ni, and Zn show strong positive skewness, implying that a few sites contribute disproportionately to overall contamination loads. Such findings emphasise the importance of targeted remediation and monitoring of high-risk zones rather than relying solely on mean concentration values. As Yang et al. [30] emphasised, KDE provides a more realistic representation of contaminant distribution than traditional parametric methods, capturing both typical and extreme concentration ranges that influence exposure risk..

Kernel Density Estimation

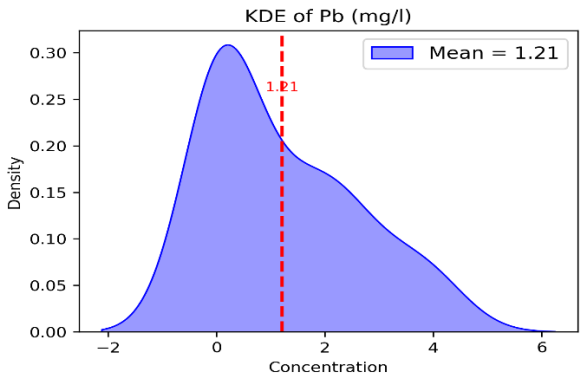

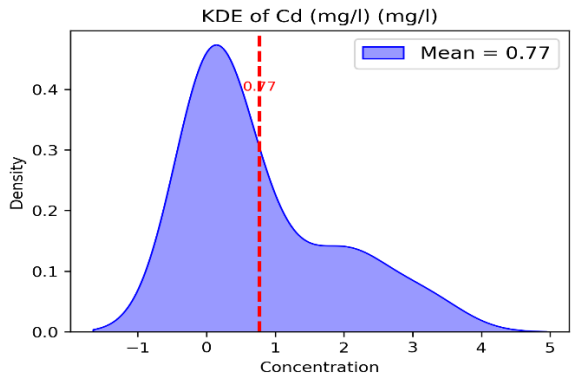

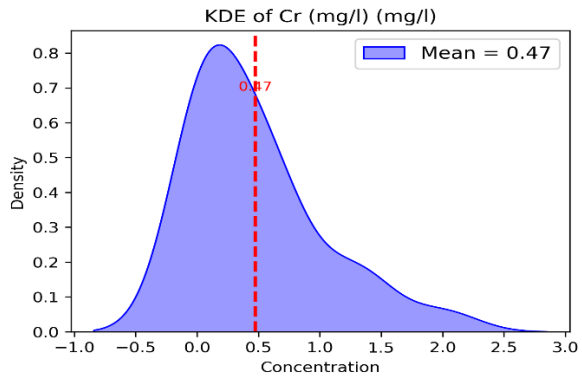

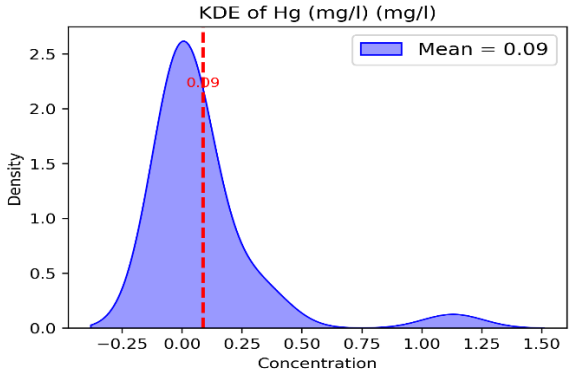

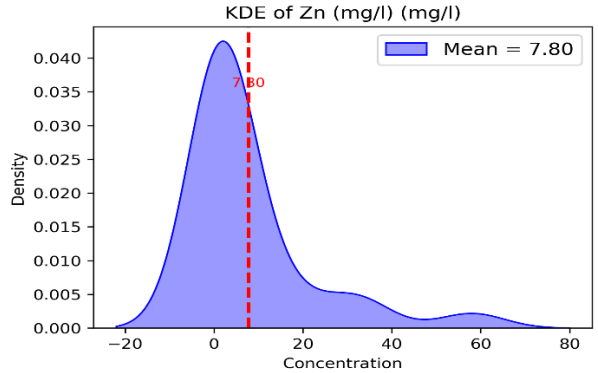

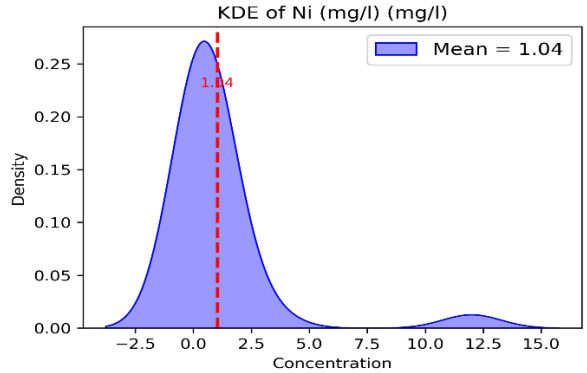

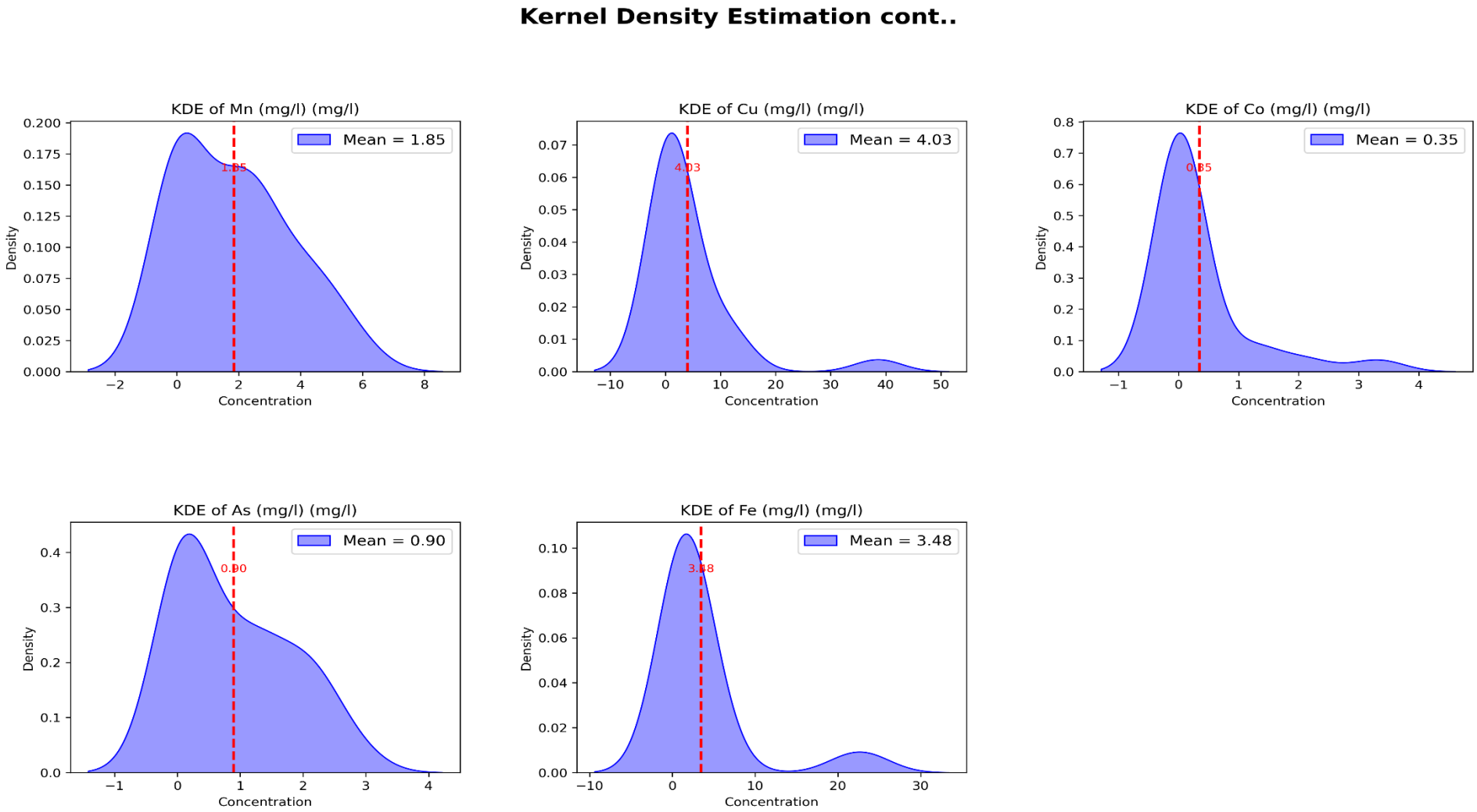

Figure 2. Kernel Density Estimation

3.1.1 *Pearson's Correlation*

From Pearson's correlation matrix presented in Figure 3, several notable positive correlations are evident. For example, Lead (Pb) shows a significant positive correlation with Cadmium (Cd) (0.55), Chromium (Cr) (0.70), Mercury (Hg) (0.70), and Zinc (Zn) (0.74). This suggests that higher concentrations of one metal may be associated with higher concentrations of the others. Likewise, Mercury (Hg) has very strong positive correlations with Zinc (Zn) (0.90) and Chromium (Cr) (0.80). These robust correlations often point to shared pollution sources or similar geochemical processes in the environment [46]. Various factors, such as industrial activities, certain waste-disposal methods, or specific geological formations, can release multiple heavy metals simultaneously, leading to their co-occurrence and the observed strong correlations. In contrast, some metals show either weak or negative correlations. For instance, Nickel (Ni) typically shows low positive correlations with most other metals, including a very weak one with Pb (0.04) and a slightly stronger one with Cr (0.20). However, Ni shows nearly no correlation with Manganese (Mn) (-0.03) or Iron (Fe) (-0.03), indicating that their concentrations are largely independent [47]. Copper (Cu) shows moderate positive correlations with Cr (0.59) and Hg (0.80), but weaker correlations with other metals. Arsenic (As) shows a strong positive correlation with Chromium (Cr) (0.59) and Manganese (Mn) (0.79), but a negative correlation with Iron (Fe) (-0.21), an important finding [48]. This negative correlation between As and Fe may result from the adsorption of arsenic onto iron oxyhydroxides under certain environmental conditions, suggesting that higher iron levels could lead to lower dissolved arsenic [36]. When comparing these observations with recent studies, the strong positive correlations among Pb, Cd, Cr, Hg, and Zn are often reported in research concerning heavy metal pollution in various environmental samples. For instance, investigations on heavy metal levels in agricultural soils typically find significant positive correlations between Cd and Zn due to their similar chemical characteristics and industrial applications [49]. Additionally, studies focused on industrial wastewater or sediments frequently demonstrate strong correlations between Cr and Ni, indicating their joint release from similar industrial activities such as electroplating or tanning [50]. The high correlation between Hg and Zn might suggest specific industrial emissions or waste streams where these metals are released together. Likewise, the relatively weak or negative correlations, such as those noticed between Nickel and Iron, align with existing literature [51]. The behavior of Iron, being a common element in the Earth's crust, often varies from that of trace heavy metals. Its presence can significantly affect the mobility and bioavailability of other metals through processes like precipitation, adsorption, and complexation [52]. The negative correlation between As and Fe, as mentioned, is a well-established phenomenon in both aquatic and soil environments, where iron oxides are key to arsenic immobilization [53]. The low correlations observed between Nickel and certain metals may indicate more varied or localized sources of Nickel, or distinct environmental processes influencing its distribution, compared to other heavy metals.

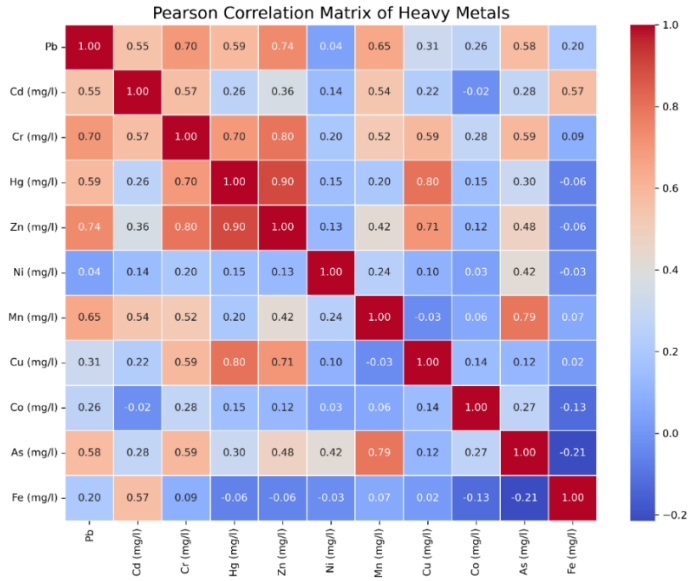

Figure 3. Pearson's Correlation

3.2 Geospatial distribution

The results indicated that the concentration of these heavy metals varies with anthropogenic activities in the area. The concentration of all the heavy metals is scaled according to the contour map legend. All concentration levels were compared to the WHO [37] acceptable limit.

3.2.1 Arsenic

Looking at the contour map data presented Figure *4*, it can be seen that the distribution of arsenic (As) in the Jalingo area follows a clear and organised pattern. The arsenic levels are not scattered randomly; instead, they show a strong directional trend. The highest concentration, peaking at 5.284 mg/l, is definitely found in the northwestern section of the sampled area, specifically around the coordinates 8.90, 11.25. This spot is a major contamination hotspot. From this northwestern centre, the arsenic levels steadily decrease as you move southeast. The contour lines illustrate this decline, with values dropping from 2.472 mg/l and 1.660 mg/l to the lowest recorded level of 0.153 mg/l in the southeastern corner, roughly at latitude 8.85 and longitude 11.45. The closely spaced contour lines, especially in the western half of the map, suggest a steep gradient, indicating that the arsenic concentration changes quickly over a relatively short distance. This findings agrees with that of Gok et al. [54].

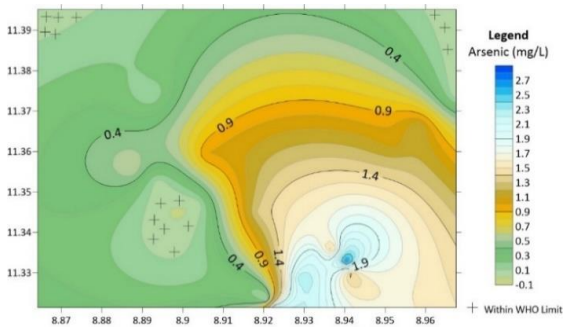

Figure 4. Spatial distribution of Arsenic in the study area

3.2.2 Cadmium

Cadmium (Cd) has a high concentration within the central part of Jalingo, based on the cardinal point. The red colouration of the contour indicates the highest concentration. The concentration is high in the Southeast and Southwest, while it tends to be low or within acceptable limits in the northeast and northwest (Figure *5*). The spatial nature of the contaminants inducates heterogeneity of anthropogenic activities [55], [56]. The sharp concentration gradients shown in the contour pattern, where levels drop dramatically from 3.2 mg/L to 0.4 mg/L while moving away from the hotspots, indicate that the contamination is not spreading much and is being strongly absorbed by the aquifer materials. This aligns with findings from Ibe et al. [57]**.**

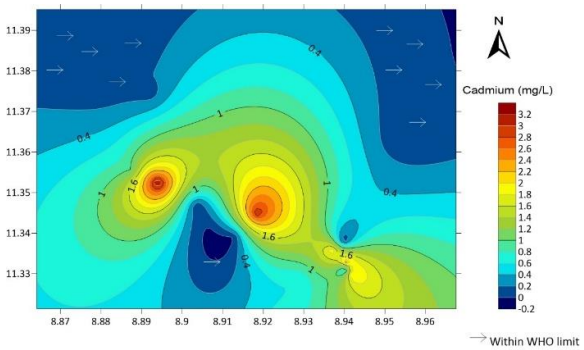

Figure 5. Spatial distribution of Cadmium in the study area

3.2.3 Chromium

Figure *6* presents a contour map of the spatial distribution of chromium across the study area. The results reveal that chromium is high in the South-west and western parts of the study area. However,

the southeast is indicated as the area with the highest contaminant level (1.6 mg/L). Meanwhile, the concentration was within the WHO-recommended limit throughout the northern and Middle East parts of the study area, as indicated by the plus symbols. All the white to deep blue colouration represents high concentration. The pattern see**n**, with high concentrations clustered in certain areas, suggests that this pollution is coming from specific sources like industrial sites, agricultural practices, and waste disposal. In contrast, the northern and middle eastern areas appear to be cleaner, indicating less human impact and better protection for the aquifer. Similar findings emerged in recent hydrogeochemical studies throughout Nigeria and other developing regions. For instance, Onwuka et al. [56] found Cr levels ranging from 0.8 to 2.1 mg/L in groundwater in Makurdi, linking these elevated levels to metal plating workshops, tannery waste, and leachate from landfills.

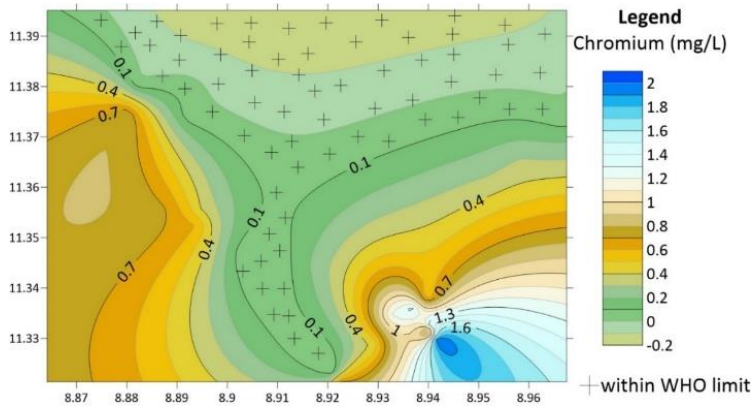

Figure 6. Spatial distribution of Chromium

3.2.4 Cobalt

The distribution of cobalt contamination across the contour shown in Figure 7 is varied, with notable concentrations in the northeast, south, southeast, and eastern regions. The high levels of cobalt in these areas, highlighted by the white-to-blue shading on the contour map, hint at possible connections to human activities like industrial runoff, vehicle emissions, metal workshops, and waste disposal. This observation aligns with Okafor et al. [4] who found an increase in cobalt levels in groundwater around industrial corridors of Onitsha and Nnewi, linking this rise to poor waste management and leaching from metal fabrication industries. Likewise, Usman et al. [58] conducted a study in Bauchi metropolis and discovered that regions near battery disposal sites and auto-mechanic workshops had cobalt levels exceeding WHO limits. The concentration pattern observed in Jalingo's mechanic village mirrors these findings, particularly the elevated levels in areas with high human activity and waste buildup. Meanwhile, in the western and a few south-eastern parts of the study area, cobalt was found to be low, indicated by the plus (+) sign. Additionally, Oyewo et al. [13] pointed out that cobalt contamination in groundwater is often worsened by unregulated artisanal practices and inadequate drainage systems that allow metals to seep into aquifers. The relatively lower cobalt levels seen in the western and some southeastern parts of the Jalingo study area could be due to less industrial and human impact.

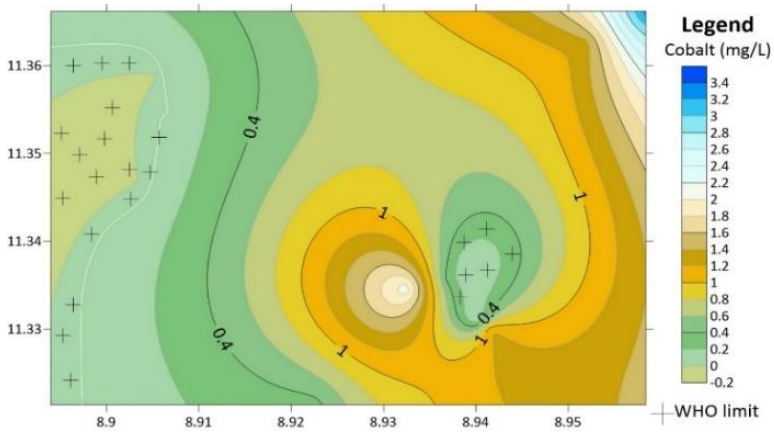

Figure 7. Spatial distribution of Cobalt

3.2.5 Copper

Figure 8 shows the spatial distribution of copper (Cu) in the study area, revealing concentrations ranging from nearly 0 to 38 mg/L. The highest levels appear in the eastern zone, indicated by closely spaced blue contours, while the central and western regions show moderate values (2–6 mg/L). This spatial pattern suggests the influence of localized pollution sources, likely linked to anthropogenic activities such as industrial discharge, waste disposal, or agricultural runoff. The uneven distribution also indicates that copper movement follows subsurface flow paths, with steep gradients to the east pointing to groundwater transport from a specific contamination source. In contrast, lower concentrations in the west may reflect dilution or attenuation processes. These Findings are consistent with earlier studies. Owamah et al. [43] reported that groundwater copper levels in the Niger Delta were highest near automobile workshops and decreased with distance due to dilution and adsorption. Similarly, Akoto [59] observed spatial variability in copper levels in Lagos groundwater, noting hotspots near waste disposal sites and industrial zones. Ahmed et al. [60] also documented elevated copper and iron levels in Hadejia Metropolis linked to human activities and hydrogeochemical conditions that enhanced metal solubility. The maximum detected concentration of 38 mg/L greatly exceeds the WHO drinking water limit of 2 mg/L, indicating severe contamination with potential public health implications. Long-term exposure to such levels may cause gastrointestinal distress, liver and kidney damage, and metal bioaccumulation in humans [32]. The moderate concentrations (2–6 mg/L) in the western and central regions likely represent secondary dispersion zones influenced by land-use practices, including copper-based agrochemicals and urban runoff. Similar multi-source contamination patterns have been reported by Jomova et al. [33] in Rivers State and by Royer and Sharma [61] in Effurun–Warri, where industrial activities and groundwater flow direction altered heavy-metal distribution.

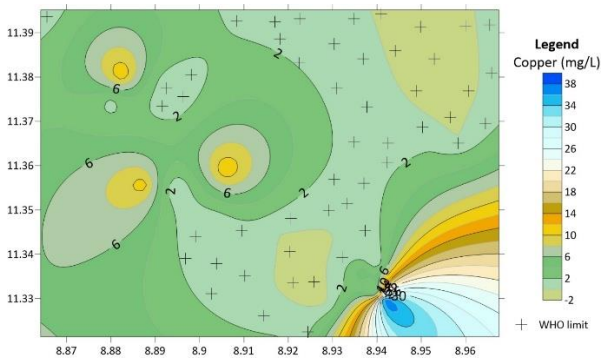

Figure 8. Spatial distribution of copper

4.2.6 Iron

Figure 9 shows the spatial distribution of iron in the study area, revealing notable variations across the site. Iron, although an essential micronutrient, becomes problematic when it exceeds the WHO limit of 0.3 mg/L [51]. The contour map indicates that several zones surpass this threshold, signalling potential contamination and the need for continuous monitoring. The highest concentrations occur in the southwestern region, represented by a white-to-blue gradient, suggesting a localised iron increase. This may arise from natural sources, such as the weathering of iron-rich minerals or anthropogenic activities including corroded pipes, waste disposal, and agricultural runoff. These observations align with previous studies. Ahmed et al. [60] reported similarly high iron levels in Hadejia Metropolis due to both geologic and human-induced factors, while Grabić et al. [34] found pronounced iron contamination in low-lying, densely populated areas of Jos, linked to human impacts. Beyond the southwestern hotspot, moderately elevated iron levels are observed elsewhere in the study area, suggesting that iron is widespread within the aquifer but varies in concentration. This uneven distribution may reflect differences in subsurface geochemistry, groundwater flow, or soil–water interactions, consistent with Akoto's findings of variable metal concentrations in Lagos groundwater [59]. Conversely, the northeastern zone, marked by plus-sign symbols, exhibits lower iron concentrations. This reduction may result from improved aquifer flushing, reduced human activity, or oxidising conditions that lead to the precipitation of iron oxides. Owamah et al. [43] similarly reported

lower dissolved iron in areas with higher recharge and oxygen levels. Overall, the pattern reflects a combination of natural geological controls and human activities. The elevated iron in the southwest may be linked to reductive dissolution of ferric minerals, while the spatial variability across the site indicates hydrogeochemical zonation, consistent with Baawain et al. [62], who noted that heavy metal distributions often form spatial gradients driven by lithology and anthropogenic influences.

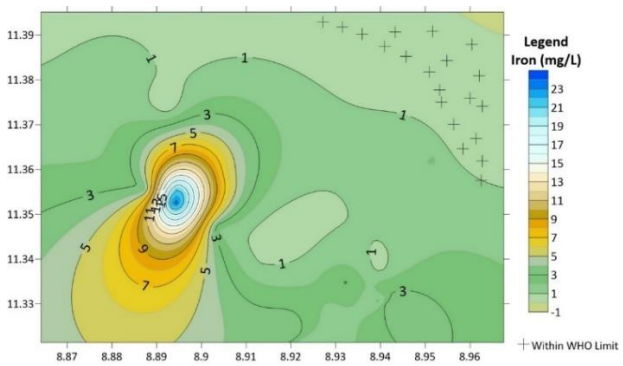

Figure 9. Spatial distribution of Iron

4.2.7 Lead

Figure 10 shows the spatial distribution of lead (Pb) in the study area, revealing major variations in concentration across the region. Lead has no biological function and is highly toxic even at very low levels; the WHO safe limit for drinking water is 0.01 mg/L, and exceeding it can cause neurological damage, kidney impairment, and developmental problems in children [37]. The contour map indicates notably high lead concentrations in the northeastern part of the area, extending westward. These yellow-to-red zones reflect severe contamination, likely originating from human activities such as waste disposal, industrial emissions, battery recycling, and vehicle-related pollution. Comparable hotspots were documented by Owamah et al. [43] in the Niger Delta near automobile and metalworking sites. Moderately elevated lead levels also appear in the central region, shown in light blue, suggesting dispersion along groundwater flow paths. These concentrations may reflect dilution or adsorption processes within the aquifer. According to Youssef et al. [63], lead mobility is influenced by pH, redox conditions, and colloidal transport, often creating spatial patterns that radiate from pollution sources. In contrast, the northwestern and southern zones, represented by deep blue colours with star symbols, show low lead concentrations that generally fall within WHO limit. These levels may correspond to cleaner recharge zones or natural geochemical conditions—such as higher alkalinity and reduced lead solubility, that inhibit contamination. Adene et al. [64] similarly observed low lead levels in less industrialised, well-flushed aquifers in Jos. Overall, the distribution pattern indicates both point-source contamination and broader hydrogeologic controls. The northeastern hotspot likely reflects a specific activity, while decreasing concentrations toward the south and west align with subsurface flow directions. Akoto et al. [59] reported similar flow-controlled metal dispersion in Lagos groundwater. The presence of additional moderate zones suggests influences from multiple non-point sources, including urban runoff and leachate infiltration.

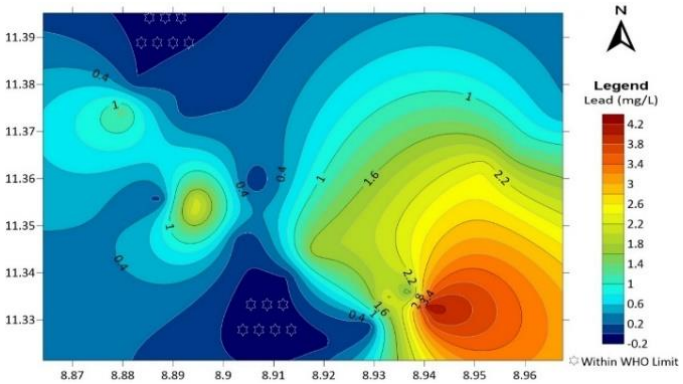

Figure 10. Spatial distribution of Lead

4.2.8 Manganese

The contour map (Figure 11) illustrates manganese (Mn) distribution in groundwater, showing strong spatial variation across the study area. The highest concentrations (4.8–5.6 mg/L) occur in the central to southeastern region, marked by red–orange colours, while moderate levels (2.4–3.6 mg/L) appear in the surrounding yellow and green zones. The lowest concentrations (below 1.0 mg/L), shown in deep blue and cyan, are found in the northwestern and southwestern areas. Since the WHO limit for Mn in drinking water is 0.4 mg/L [36], much of the area exceeds this threshold. The central–southeastern hotspot suggests localised enrichment, likely influenced by both natural processes, such as the dissolution of Mn-rich minerals under reducing aquifer conditions, and anthropogenic activities including waste leaching, industrial discharge, or agricultural runoff. Similar patterns have been reported in Nigerian groundwater studies: Kabir et al. [65] linked high Mn in Hadejia Metropolis to natural weathering and human contributions, while Mohan et al. [36] observed elevated Mn in industrialised parts of Jos Metropolis compared to less disturbed zones. The spatial gradient indicates that manganese transport follows groundwater flow paths, with concentrations decreasing outward through processes such as dilution, dispersion, and adsorption onto aquifer materials. Akoto [59] noted comparable declines in Lagos aquifers, where geochemical interactions and carbonate buffering reduced Mn levels away from industrial centres. Conversely, the low concentrations in the northwest and southwest suggest cleaner recharge zones or oxidising conditions that promote the formation of insoluble Mn oxides, limiting mobility, an effect also observed by Owamah et al. [43] in the Niger Delta. The widespread exceedance of WHO limits poses public health risks, as prolonged exposure to high Mn can cause neurological and cognitive effects, especially in children [66]. This pattern aligns with broader findings that both natural geochemistry and human activities shape groundwater metal variability in Nigeria [67].

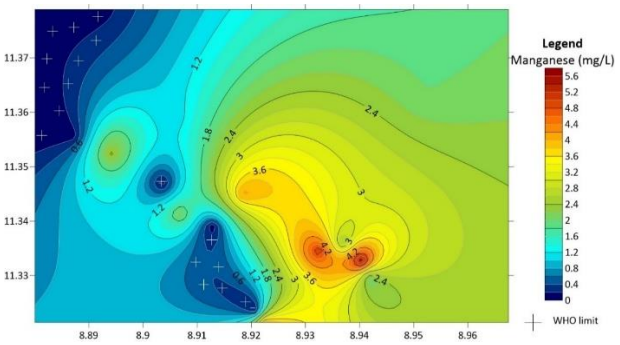

Figure 11. Spatial distribution of Manganese

4.2.9 Mercury

The contour map (Figure 12) illustrates spatial variability in mercury (Hg) concentrations across the study area, with values ranging from 0.0 to 1.05 mg/L. The highest levels occur in the southeastern corner, shown in yellow to light blue, where concentrations exceed 0.45 mg/L. In contrast, the central, northern, and much of the northwestern regions marked in green and indicated by plus signs remain within the WHO limit of 0.001 mg/L [68]. This pattern points to localised contamination driven by human activities and hydrogeochemical conditions. The southeastern hotspot likely reflects pollution from industrial discharges, waste burning, or improper disposal of mercury-containing materials such as batteries, paints, and electronics. Comparable localised enrichment was reported by Zhu et al. [69] in Ado-Ekiti, where poor waste management led to Hg infiltration into shallow aquifers, and by Ezra et al. [34] in Minna, where artisanal gold mining contributed to elevated groundwater mercury. Natural contributions may also play a role in the southern and southeastern zones. Under favourable redox conditions, the weathering of mercury-bearing minerals or sulfide ores can release Hg into groundwater, whereas reducing environments enhance solubility by forming Hg–S complexes. Jomova et al. [33] observed similar geochemical controls on mercury distribution in the Enugu Basin. Conversely, the northern and western parts show low to negligible Hg levels, likely due to limited contamination, active recharge, and permeable aquifer units that promote flushing patterns consistent with findings by Omoregie et al. [70] in Nsukka. The elevated Hg concentrations in the southeast raise serious environmental and public health concerns. Mercury is a potent neurotoxin associated with neurological,

renal, and developmental harm, especially with long-term exposure. Communities consuming Hg-contaminated groundwater face risks of poisoning and bioaccumulation in food chains [34]. The observed distribution aligns with broader evidence that mercury contamination tends to be patchy, source-dependent, and strongly shaped by land use and hydrogeological factors [71].

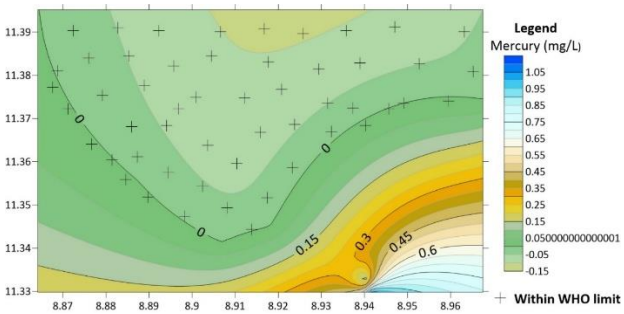

Figure 12. Spatial distribution of Mercury

4.2.10 Nickel

Figure 13 illustrates the spatial distribution of nickel (Ni) in groundwater, with concentrations ranging from below 1.0 mg/L to about 11.5 mg/L. These values far exceed the WHO drinking water limit of 0.02 mg/L [37]. The highest concentrations occur in the south-central region, shown by red–orange colours, forming a distinct contamination hotspot. Nickel levels decrease progressively outward, with the green–blue zones in the northwestern and northeastern areas falling within WHO guidelines, marked by star symbols. The southern hotspot suggests a localised pollution source influenced by both human and natural factors. Possible contributors include industrial waste disposal, leachates from metal scraps, and agricultural runoff containing nickel compounds. Natural sources may also contribute through the weathering of nickel-bearing minerals such as olivine and pyrrhotite under mildly reducing conditions. Similar patterns have been observed elsewhere in Nigeria: Saha and Gupta [72] reported elevated nickel levels near industrial zones in Ogun State, while Neider et al. [73] linked high nickel in Aba groundwater to industrial runoff and leaching from solid waste and metallurgical residues. The strong contrast between high- and low-nickel zones indicates that Ni is likely migrating along permeable pathways or fractures, consistent with findings by Zech et al. [74], who observed nickel and chromium plumes moving along preferential groundwater flow paths in lateritic aquifers. Overall, the distribution pattern reflects the combined influence of hydrogeochemical processes and human activities. The concentration hotspot's proximity to potential pollution sources and groundwater flow routes underscores the role of land-use practices and aquifer dynamics. This elevated nickel poses notable health risks, including dermatitis, cardiovascular problems, and carcinogenic effects with long-term exposure [75].

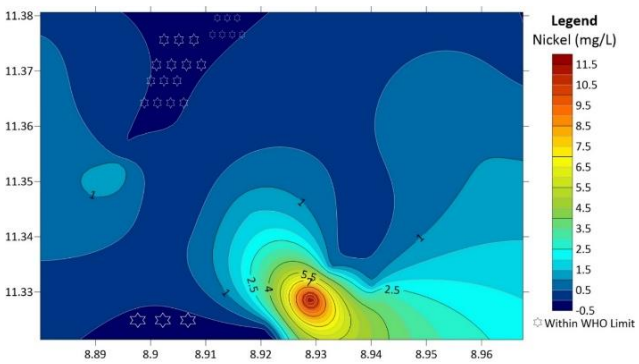

Figure 13. Spatial distribution of Nickel

4.2.11 Zing

Figure 4.14 illustrates the spatial distribution of zinc (Zn) in groundwater, showing concentrations ranging from below 5 mg/L to nearly 60 mg/L. These values exceed the WHO drinking water limit of 3 mg/L for zinc, indicating that a substantial portion of the study area contains unsafe levels. The highest concentrations appear in central zones, while lower values occur along the map's

edges, suggesting areas less affected by human activities. The elevated zinc levels likely stem from both point and diffuse sources. Possible contributors include industrial discharges, corrosion of galvanised pipelines, and road runoff, where tyre wear releases significant amounts of zinc [32]. Similar patterns of uneven heavy-metal distribution in groundwater were reported by Chen et al. [76], who linked elevated concentrations to ageing industrial facilities and leaking infrastructure in urban aquifers. The implications of this distribution are notable. From a health perspective, communities relying on groundwater from high-concentration zones may face risks such as nausea, stomach discomfort, and long-term copper deficiency associated with excessive zinc intake [77]. Environmentally, elevated zinc can disrupt aquatic habitats and impair ecosystem functioning. The map effectively pinpoints contamination hotspots, making it a valuable tool for targeted remediation. The coexistence of compliant and non-compliant zones across a relatively small area highlights the complexity of urban hydrogeology. Factors such as land-use patterns, soil characteristics, and subsurface flow dynamics contribute to this variability. Adimalla [78] similarly found that zinc and lead levels can shift sharply over short distances, reinforcing the need for detailed spatial monitoring. Such precision allows mitigation measures such as pollution source control or the installation of permeable reactive barriers to be implemented exactly where they are most effective in protecting both human health and the environment.

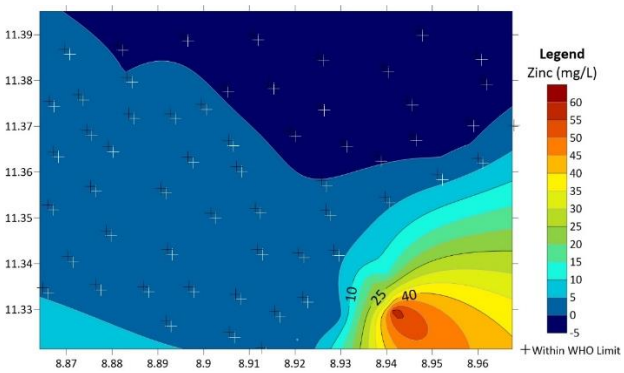

Figure 14. Spatial distribution of Zinc

4.3 Heavy Pollution Index Risk Factor (HPI-RF)

The Heavy Metal Pollution Index (HPI), also known as the Heavy Metal Pollution Index, provides a clear numerical assessment of water quality relative to heavy metal concentrations. This index consolidates complex information from various heavy metal analyses into a single, comprehensible figure that indicates the level of water contamination. The risk factor (RF) associated with the HPI is classified into three categories: low, medium, and high risk. A map provides essential spatial insights into the analysis of heavy metal pollution, based on risk classifications derived from groundwater samples collected in and around Jalingo, along with their corresponding geographic coordinates. To predict the risk factor, a Support Vector Machine (SVM) algorithm was implemented to build a model that forecasts the HPI-RF within a Python environment in Anaconda. The results indicate that out of 25 sampling points, 12 are classified as high risk, 13 as low risk, and 2 as medium risk. The high-risk locations fall within the latitude range of 8.85 to 8.90 and the longitude range of 11.25 to 11.35 (Figure 7).

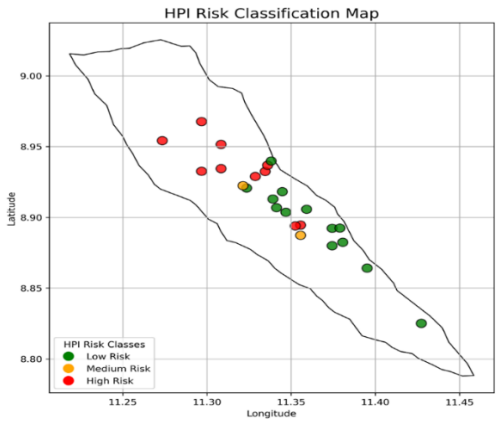

Figure 7. Model Risk classification

The model demonstrated strong accuracy of 0.875 (87.5%), indicating it correctly predicted the class for 7 out of 8 test samples, as illustrated in the confusion matrix in Figure 16. However, both the confusion matrix and the classification report highlight notable challenges related to class imbalance and the model's failure to predict one of the classes. This issue arose because only two medium-risk areas were present within the study area, despite three risk categories. The limited data for medium-risk prediction contributed to the model's errors.

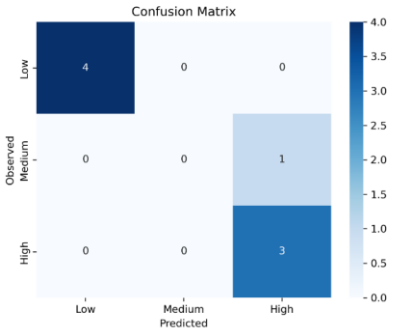

Figure 16. Matrix showing model performance

4 CONCLUSIONS

The assessment of groundwater quality across the study area reveals widespread contamination by multiple heavy metals, many of which exceed WHO drinking-water limits. Spatial analyses show distinct hotspots for Pb, As, Cu, Ni, Mn, Hg, Cr, Co, and Zn, largely concentrated in zones influenced by industrial activities, waste disposal, agricultural runoff, leaking infrastructure, and natural geochemical processes. The distribution patterns indicate both point-source pollution and flow-controlled dispersion along permeable aquifer pathways. Statistical correlations further suggest that many metals originate from common anthropogenic sources. The Heavy Pollution Index Risk Factor (HPI-RF) and SVM modelling classify several locations as high-risk, confirming that groundwater in parts of the study area is unsafe for consumption without treatment. Overall, the findings highlight significant public-health concerns, ecological risks, and the urgent need for improved groundwater protection. These results suggest that the groundwater in this region is largely unsafe for direct human use. Prolonged exposure poses significant public health risks, particularly neurological, kidney, and cancer-related issues. To alleviate these risks, urgent actions are required, including enhanced water quality monitoring, improved waste management practices, remediation efforts, and community education programs. Furthermore, long-term strategies for sustainable groundwater management and pollution control should be prioritised to ensure water safety for Jalingo's growing population.

CONTRIBUTION

All the Authors contributed to the field data collection process. F. G. Ngasoh analysed the data; B. A. Ankidawa compiled the manuscript, and B R. Burmamu proofread it.

ACKNOWLEDGEMENTS

This research was funded by the Tertiary Education Fund (TEdFund). The Authors, therefore, wish to acknowledge the Nigeria TEdFund for their fellowship support and sponsorship.

CONFLICT OF INTEREST

All the Authors have unanimously agreed on everything that concerns the paper, and there is no conflict of interest.

REFERENCES

1. Pradesh, A., Krishna, A.K., Satyanarayanan, M. and Govil, P.K. (2009). Assessment of heavy metal pollution in water using multivariate statistical techniques in an industrial area: A case study from Patancheru, Medak District. *Jour. Hazard. Mater*., vol. 167, no. 12, pp. 366-373.
2. Abebe, L.S., Chen, X. and Sobsey, M.D. (2023). Global groundwater contamination: Trends, sources, and mitigation strategies. *J. Environ. Manage*., vol. 330, pp. 117-135.
3. Sharma, R.K. and Walia, M. (2017). Heavy metal toxicity in aquatic ecosystems: A review of sources, effects, and remediation strategies. *Water, Air, Soil Pollut*., vol. 228, no. 10, pp. 401-425, doi: https://doi.org/10.1007/s11270-017-3585-0.
4. Ogueri, E., Okafor, C. and Nwachukwu, M. (2018). Heavy metal persistence in aquatic systems: Ecological and public health implications. *J. Environ. Heal. Sci*., vol. 16, no. 2, pp. 78-92.
5. Abdelrahman, K., Fnais, M., Ibrahim, E. and Qaysi, S. (2025). Heavy metal bioaccumulation in aquatic ecosystems: Mechanisms and health implications. *Environ. Sci. Pollut. Res*., vol. 32, no. 4, pp. 1123-1145, doi: https://doi.org/10.1007/s11356-024-34567-9.
6. Yohanna, A., Musa, N., Balogun, F.A., Agada, E.A., Adamu, A. and Galumje, S.S. (2022). Investigation of Groundwater Contamination in Some Selected Areas of Bogoro and Environs, North-East Nigeria. *Fudma J. Sci*., vol. 6, no. 1, pp. 358-367.
7. Liosis, C., Papadopoulos, A. and Karvelas, E. (2021). Non-biodegradability of heavy metals: A review of toxicity mechanisms and global regulatory frameworks. *Environ. Res*., vol. 200, pp. 111-125, doi: https://doi.org/10.1016/j.envres.2021.111125.
8. Zhang, Y., Li, H. and Tang, C. (2023). Neurological and carcinogenic effects of heavy metal exposure: A meta-review. *J. Toxicol*., vol. 11, no. 3, pp. 123-267, doi: https://doi.org/10.1155/2023/4567890.
9. Olawade, D.B., Wada, O.Z. and Afolabi, O.T. (2024). Anthropogenic sources of heavy metal pollution in water resources: A global review. *Environ. Challenges*, vol. 14, pp. 100-115, doi: https://doi.org/10.1016/j.envc.2023.100115.
10 Mititelu, M., Udeanu, D.I., Nedelescu, M., Neacsu, S.M. and Goumenou, M. (2025). Chronic heavy metal exposure and human health risks: A meta-analysis. *Toxicol. Reports*, vol. 12, pp. 45-59.
11. Shen, J., Liu, E., Zhu, Y. and Gao, Z. (2019). Natural and anthropogenic sources of heavy metals in aquatic systems: A geochemical perspective. Environ. *Geochem. Health*, vol. 41, no. 6, pp. 2759-2779, doi: https://doi.org/10.1007/s10653-019-00393-5.
12. Rehman, K., Fatima, F., Waheed, I. and Akash, M.S.H. (2017). Prevalence of exposure to heavy metals and their impact on human health. *Environ. Sci. Pollut. Res*., vol. 25, no. 10, pp. 9283-9298, doi: https://doi.org/10.1007/s11356-017-1125-5.
13. Oyewo, O.A., Adeniyi, A. and Onyango, M.S. (2021). Resistance of heavy metals to natural degradation processes in water systems. *Chemosphere*, vol. 285, pp. 131-145, 2021, doi: https://doi.org/10.1016/j.chemosphere.2021.131145.
14. Ali, H., Khan, E. and Ilahi, I. (2019). Environmental chemistry and ecotoxicology of hazardous heavy metals: Environmental persistence, toxicity, and bioaccumulation. *J. Chem*., vol. 2019, pp. 234-245, doi: https://doi.org/10.1155/2019/6730305.

15. Karnwal, A. and Malik, T. (2024). Industrial effluents and climate change: Synergistic impacts on aquatic heavy metal pollution. *Sci. Total Environ*., vol. 912, pp. 169-182.

16/. Senoro, D.B., Tabelin, C.B. and Maglambayan, V.B. (2022). Heavy metal contamination in groundwater: A silent threat to sustainable development. *J. Hazard. Mater*., vol. 442, pp. 130-143, doi: https://doi.org/10.1016/j.jhazmat.2022.130143.

17. Alemu, U. (2019). Evaluating the Environmental Impacts of Industrialization and Urbanization on Groundwater Quality: A Comprehensive Review of Methodological Approaches in Ethiopia. *IntechOpen J*., vol. 11, no. 1, pp. 1-14.

18. Wong, W.L., Emre, M. and Talukdar, G. (2024). Groundwater Contamination by Heavy Metals in Malaysia: Sources, Transport, and Remediation Strategies. *Trop. Environ. Biol. Technol*., vol. 2, no. 2, pp. 93-105.

19. Benson, N.U., Adedapo, A.E. and Fred-ahmadu, O.H. (2018). New ecological risk indices for evaluating heavy metals contamination in aquatic sediment: A case study of the Gulf of Guinea. *Reg. Stud. Mar. Sci.*

20 Karaouzas, I., Kapetanaki, N., Mentzafou, A., Kanellopoulos, T.D. and Skoulikidis, N. (2021). Heavy metal contamination status in Greek surface waters: A review with application and evaluation of pollution indices. *Chemosphere*, vol. 263, no. 2, pp. 1-5.

21. Qingjie, G. and Jun, D. (2008). Calculating Pollution Indices by Heavy Metals in Ecological Geochemistry Assessment and a Case Study in Parks of Beijing. *J. China Univ. Geosci*., vol. 19, no. 3, pp. 230-241.

22. Bsiwas, P.K., Uddin, N., Alam, S., Us_Sakib, T., Sultana, S. and Ahmed, T. (2017). Evaluation of Heavy Metal Polution indices in irrigiation and drinking water system of Barapukuria coal mine area, Bangladesh. *Am. J. Water Resour*., vol. 5, no. 5, pp. 146-151.

23. Madhav, V., Dipak, W., Panaskar, B., Vitthal, S., Satyajit, M. and Gaikwad, K. (2018). Health risk assessment of heavy metal contamination in groundwater of Kadava River Basin, Nashik, India. *Model. Earth Syst. Environ*., vol. 23, no. 2, pp. 1-12.

24. National-Bureau-of-Statistics (2024). Nigeria: Administrative Division, State and Local Government Areas. *National Population Commission. Accessed*: Mar. 03, 2024. [Online]. Available: https://citypopulation.de/en/nigeria/admin/NGA035__taraba/.

25. Ngasoh, F.G., Akindawa, B.A., Burmamu, B.R. and Usman, M.N. (2025). Assessment of Aquifer Protective Capacity around Contamination Vulnerable Areas in Jalingo, Taraba State, Nigeria. *Taraba J. Eng. Technol*., vol. 5, no. 1, pp. 36-44.

26. Tsunatu, D.Y., Kurutsi, D.S., Tickson, T.S. and Bingari, M.S. (2016). Assessment of Some physico-chemical parameters of Nukkai River tributries, Jalingo, Nigeria. *FUW Trends Sci. Technol. Journa*, vol. 1, no. 2, pp. 427-432.

27. Nandomah, S. and Tetteh, I.K. (2023). Potential ecological risk assessment of heavy metals associated with abattoir liquid waste: A narrative and systematic review. *Heliyon*, vol. 9, no. 8, p. e17359.

28. Gleeson, T., Befus, K.M., Jasechko, S., Luijendijk, E. and Cardenas, M.B. (2016). The global volume and distribution of modern groundwater. *Nat. Geosci*., vol. 9, no. 2, pp. 161-164.

29. Chutia, D., Kataki, S. and Kataki, A.S. (2025). Index-Based Evaluation (IBE) and Geospatial Mapping of Heavy Metal Contamination in Groundwater of an Industrially Influenced Peri-Urban Area of Guwahati, Assam; India. *J. Environ. Public Heal*., vol. 11, no. 1, pp. 167-186.

30. Yang, X., Ng, W., Wong, B.S.E., Baeg, G.H., Wang, C.H. and Ok, Y.S. (2019). Characterization and ecotoxicological investigation of biochar produced via slow pyrolysis: effect of feedstock composition and pyrolysis conditions. *J. Hazard. Mater*., vol. 365, no. 2, pp. 178-185.

31. Wang, Z., Gao, Y., Xu, X., Dong, W. and Jiang, T. (2023). Risk Classification Assessment and Early Warning of Heavy Metal Contamination in Meat Products. *Sustain*., vol. 15, no. 21, pp 1-18.

32. Adeel, A., Gaikwad, N., Chougale, S., Sarkale, P., Bhosale, P. and Jadhav, A. (2022). Concerning Human Health Risks of Trace Elements Contamination in Groundwater Sources nearby the Arabian Sea, Malvan Coastal Area, India. *YMER*, vol. 21, no. 8, pp. 85-104.

33. Jomova, K., Alomar, S.Y., Nepovimova, E., Kuca, K. and Valko, M. (2025). Heavy metals: toxicity and human health effects. *Springer Berlin Heidelberg*, vol. 99, no. 1, 153-209.

34. Vivan, E.L., Eziashi, A.C., Binbol, N.L. and Ameso, V.C. (2023). Hydro-geochemical characterization and modeling of groundwater in Chikun Local Government Area of Kaduna state, Nigeria. *Water Pract. Technol*., vol. 18, no. 12, pp. 3203-3220.

35. Das K.K., Reddy R., Bagoji I. and Das S. (2019). Primary concept of nickel toxicity – an overview. *Journal of Basic Clinical Phys. Pharmacol.* vol. 30, no. 2, pp. 141-152.

36. Mohan, I., Jasrotia, R., Dhar, S. and Bhau, B.S. (2024). Pollution indices and correlation of heavy metals contamination in the groundwater around brick kilns in Jammu and Kashmir, India. *Heliyon*, vol. 10, no. 6, p. e27869.

37. WHO (2022). Guidelines for drinking-water quality: Fourth edition incorporating the first and second addenda. *World Heal. Organ*., 2022, [Online]. Available: https://www.who.int/publications/i/item/9789240045064.

38. Khan, M.S., Rahman, M.A. and Alam, S. (2023). Transfer of toxic metals from contaminated irrigation water to crops in South Asia: Implications for food safety and health. *Environ. Monit. Assess*., vol. 195, no. 2, pp. 155-170.

39. Akan, J.C., Abdulrahman, F.I., Sodipo, O.A. and Chiroma, Y.A. (2013). Distribution of heavy metals in the liver, kidney and muscle of various fish species from Lake Chad, Nigeria. *World J. Anal. Chem*., vol. 1, no. 4, pp. 70-76.

40. Amaechi M. and Onwuka, S.U. (2021). Determination of the presences and level of heavy metals in soils of automobile workshops in Awka, Anambra state. *Int. J. Environ. Pollut. Res*., vol. 9, no. 3, pp. 167-186.

41. Tchounwou, P.B., Yedjou, C.G., Patlolla, A.K. and Sutton, D.J. (2012). Heavy metal toxicity and the environment. *Mol. Clin. Environ. Toxicol*., pp. 133-164.

42. Alaekwe, I.O., Ani, N.C. and Ezeogu, V.O. (2019). Heavy Metals Accumulation in Soils from Mechanic Workshops Within Gusau Town. *Int. J. Sci. Glob. Sustain*., vol. 5, no. 1, p. 1-5.

43. Owamah, H.I. and Izinyon, O.C. (2015). Evaluation of groundwater quality around solid waste dumpsites in Delta State, Nigeria. *J. Appl. Water Eng. Res*., vol. 3, no. 1, pp. 22-31.

44. Akpan, U.G., Idris, M.B. and Bature, A.A. (2020). Hydrogeochemical characteristics of groundwater in Jalingo and environs, Northeastern Nigeria. *J. Environ. Hydrol*., vol. 28, no. 3, pp. 12-25.

45. Ogunyemi, A.O., Adegbite, O. and Taiwo, K. (2022). Hydrogeochemical controls on iron mobility in tropical groundwater systems. *J. Contam. Hydrol*., vol. 243, no. 10, pp. 39-44.

46. Memon, M., Ghanghro, A.B. and Bhutto, A.A. (2021). Assessment of heavy metals in agricultural soils irrigated with municipal wastewater in Pakistan. *Environ. Monit. Assess*., vol. 193, no. 6, pp. 1-13.

47. Aljuhaimi, F., Akçay, D., Fatma, K., Yılmaz, G., Ali, I. and Ahmed, M. (2025). Quantitative Determination of Minerals and Toxic Elements Content in Tropical and Subtropical Fruits by Microwave - Assisted Digestion and ICP - OES. *Biol. Trace Elem. Res*., vol. 203, no. 3, pp. 1676-1684.

48. Liu, F., Li, M., Lu, J., Lai, Z., Tong, Y. and Wang, M. (2021). Trace Metals (As, Cd, Cr, Cu, Hg, Ni, Pb, Zn) and Stable Isotope Ratios (δ 13 C and δ 15 N) in Fish from Wulungu Lak,

Xinjiang, China. *International Journal of Environmental Research and Public Health.* vol. 18, pp. 1-18.

49. Wei, B. and Yang, L. (2010). A review of heavy metal contaminations in urban soils, roadsides and urban dusts. *Environ. Pollut*., vol. 158, no. 10, pp. 2272-2287.

50. Bhuyan, M.S., Islam, S.B., Bashar, M.Z., Ferdous, S.F. and Rahman, M.M. (2020). Assessment of heavy metal contamination in agricultural soil and its implications on crop quality in an industrial area of Bangladesh. *Environ. Sci. Pollut. Res*., vol. 27, no. 19, pp. 23964-23977.

51. Rai, S., Singh, P.K., Mankotia, S., Swain, J. and Satbhai, S.B. (2020). Iron homeostasis in plants and its crosstalk with copper, zinc, and manganese. Plant Stress, vol. 1, p. 100008.

52. Alloway, B.J. (2013). Trace Metals and Metalloids in Soils and Their Bioavailability. *In Heavy Metals in Soils, Springer Science & Business Media*, 832p.

53. Mohan, D. and Pittman, C.U. (2017). Arsenic removal from water/wastewater using adsorbents—A critical review. *J. Hazard. Mater*., vol. 1-2, pp. 1-53.

54. Gök, G., Tulun, Ş. and Çelebi, H. (2024). Mapping of heavy metal pollution density and source distribution of campus soil using geographical information system. *Sci. Rep*., vol. 14, pp. 1-18.

55. Ho, N. (2022). Assessment of the Effects of Leachates on Groundwater Quality in Igwuruta, Ikwerre Local Government Area of Rivers State, Nigeria Nwankwoala HO*, Onyughel O and Udom GJ *Corresponding author. *J. Eng. Appl. Sci. Technol*., vol. 4, no. 3, pp. 1-8.

56. Onwuka, S.U., Ejezie, E.C. and Ekeocha, N.E. (2023). Assessment of groundwater contamination by heavy metals in Makurdi and environs, north-central Nigeria. *Appl. Water Sci*., vol. 13, no. 6, pp. 197–212.

57. Ibe, K.M., Egbueri, J.C. and Nwankwo, F.O. (2021). Hydrogeochemical assessment of heavy metal pollution in groundwater around industrial and waste disposal zones in southeastern Nigeria. *Environ. Earth Sci*., vol. 80, no. 9, pp. 381-397.

58. Usman, A.A., Ibrahim, S. and Garba, M. (2022). Assessment of heavy metals in groundwater around automobile workshops in northern Nigeria. *Environ. Monit. Assess*., vol. 194, no. 2, pp. 134-146.

59. Akoto, O., Samuel, A., Gladys, L. and Addae, O. (2022). Assessment of groundwater quality from some hostels around Kwame Nkrumah University of Science and Technology. *Sci. African*, p. e01361.

60. Ahmed, A.A., Aboh, H.O. and Alhassan, U. (2019). Hydraulic conductivity estimation from vertical electrical sounding data: Case study from parts of the Chad Basin, Northeastern Nigeria. *Environ. Geol*., vol. 58, no. 7, pp. 1551-1556.

61. Royer, A. and Sharman, T. (2022). Copper Toxicity. [Online]. Available: http://www.ncbi.nlm.nih.gov/books/NBK557456/.

62. Baawain, M.S., Al-Futaisi, A.M., Ebrahimi, A. and Omidvarborna, H. (2018). Characterizing leachate contamination in a landfill site using Time Domain Electromagnetic (TDEM) imaging, *J. Appl. Geophys*., vol. 151, pp. 73-81.

63. Youssef, A.M. and Omer, A.A. (2011). land use maps to assess environmental hazards: Sohag, upper Egypt Geotechnical investigation of sewage wastewater disposal sites and use of GIS land use maps to assess environmental hazards: Sohag , upper Egypt. *Arab J. Geosci*., vol. 37, no. 12, pp. 42-84.

64. Adene, I.C., Oloye, T., Akinsorotan, A., Afolabi, D. and Obilana, O. (2023). Effect of Abattoir Effluent on Some Heavy Metals and Physico-Chemical Parameters of Ta'Jan Water in Ogbagi Akoko, Ondo State. *Int. J. Res*., vol. 10, no. 12, pp. 97-104.

65. Kabir, M.A., Chowdhury, S. and Rahman, M. (2022). Behaviour of manganese in contaminated groundwater under varying hydrogeochemical conditions. *Environ. Monit. Assess*., vol. 194, no. 2, pp. 115-128.

66. Lin, J., Zhang, Q. and Zhao, L. (2022). Long-term migration and geochemical controls of manganese in alluvial aquifers. *Sci. Total Environ*., vol. 838, no. 5, pp. 60-64.

67. Nwankwo, O.C., Adebayo, A.M. and Yusuf, T.K. (2024). Groundwater quality degradation from manganese plume migration in tropical aquifer systems. *Groundw. Sustain*. Dev., vol. 22, no. 10, pp. 12-57.

68. United Nations Environment Programme (2023). Global mercury assessment 2023: Sources, emissions, releases and environmental transport. *United Nations Environment Programme*, Available: https://www.unep.org/resources/global-mercury-assessment.

69. Zhu, M., Li, B. and Liu, G. (2022). Groundwater risk assessment of abandoned mines based on pressure-state-response — The example of an abandoned mine in southwest China. *Energy Rep*., vol. 8, no. 2, pp. 10728-10740.

70. Omoregie, E.O., Ibrahim, M.T. and Nwosu, E.A. (2024). Mercury plume behaviour in heterogeneous aquifers: Modelling and field implications. *Environ. Earth Sci.*, vol. 83, no. 2, pp. 188-203.

71. Nriagu, J., Basu, N. and Chileshe, J. (2022). Mercury and lead exposure from informal industries in sub-Saharan Africa. *Environ. Res*., vol. 204, pp. 1119-65.

72. Saha, R. and Gupta, P. (2021). Hydrogeochemical behaviour and risk assessment of nickel in groundwater near industrial zones. *J. Environ*., vol. 294, pp. 113-298.

73. Nader, A., El-Shanhorey, N. and Barakat, A. (2020). Effect of Nickel in the Irrigation Water and Foliar Applied Malic Acid on Vegetative Growth, Flowering and Chemical Composition of Salvia splendens Plant. *Sci. J. Flowers Ornam. Plants*, vol. 7, no. 4, pp. 483-499.

74. Zech, A., Dietrich, P., Attinger, S. and Teutsch, G. (2021). A field evidence model: How to predict transport in heterogeneous aquifers at low investigation level. *Hydrol. Earth Syst. Sci*., vol. 25, no. 1, pp. 1-15.

75. Kundu, S., Banerjee, R. and Mukherjee, S. (2024). Long-term transport dynamics of nickel contamination in sandy aquifers. *Environ. Adv*., vol. 15, no. 10, pp. 63-98.

76. Chen, L., Ma, T., Wang, Y. and Zheng, J. (2020). Health risks associated with multiple metal (loid) s in groundwater: A case study at Hetao Plain, northern China. *Environ. Pollut*., vol. 263, p. 114562.

77. Behtash, F. Abedini F., Amadi H., Mosavi S.V. and Ahgaee A. (2022). Zinc Application Mitigates Copper Toxicity by Regulating Cu Uptake, Activity of Antioxidant Enzymes, and Improving Physiological Characteristics in Summer Squash. *Antioxidants*, vol. 11, no. 9, pp. 1-14.

78. Adimalla, N. (2022). Application of GIS to evaluate the groundwater quality for drinking purposes in semiarid region of Telangana state, India. *In Groundwater contamination in Coastal Aquifer*, Chapter 15, pp. 191-200. doi: https://doi.org/10.1016/B978-0-12-824387-9.00006-2.